

Changes of collagen and nicotinamide adenine dinucleotide in human cancerous and normal prostate tissues studied using native fluorescence spectroscopy with selective excitation wavelength

Yang Pu

City College of the City University of New York
Institute for Ultrafast Spectroscopy and Lasers
Departments of Electrical Engineering
160 Convent Avenue
New York, New York 10031

Wubao Wang

Guichen Tang

Robert R. Alfano

City College of the City University of New York
Institute for Ultrafast Spectroscopy and Lasers
Department of Physics
160 Convent Avenue
New York, New York 10031

Abstract. The fluorescence spectra of human cancerous and normal prostate tissues obtained by the selective excitation wavelength of 340 nm were measured. The contributions of principle biochemical components to tissue fluorescence spectra were investigated using the method of multivariate curve resolution with alternating least squares. The results show that there is a reduced contribution from the emission of collagen and increased contribution from nicotinamide adenine dinucleotide (NADH) in cancerous tissues as compared with normal tissue. This difference is attributed to the changes of relative contents of NADH and collagen during cancer development. This research may present a potential native biomarker for prostate cancer detection. © 2010 Society of Photo-Optical Instrumentation Engineers. [DOI: 10.1117/1.3463479]

Keywords: fluorescence spectroscopy; selective excitation; optical biopsy; biochemical component in tissue; changes of relative contents of collagen and NADH; prostate cancer detection; multivariate curve resolution with alternating least squares (MCR-ALS).

Paper 10113RR received Mar. 5, 2010; revised manuscript received May 19, 2010; accepted for publication May 21, 2010; published online Jul. 23, 2010; corrected Jul. 30, 2010.

1 Introduction

Prostate cancer is the most common cancer in American men.¹ Since the first report on the laser-induced fluorescence from biological tissues in the 1980s by Alfano's group,^{2,3} fluorescence spectroscopy has been widely used for the diagnostic purpose of cancer, which has been called an optical biopsy. During the development from benign prostatic hyperplasia to premalignant (dysplastic) and malignant stages, prostate cells undergo proliferations and death, which modify biochemical contents.⁴ Additionally, the connective tissue frameworks of prostate tissue can be impaired during cancer evolution.⁵ Such alterations of tissue biochemistry⁴ and morphology⁵ may be revealed in the tissue fluorescence.⁶ Although there is significant experimental evidence suggesting the differences of native fluorescence spectra between cancerous and normal tissues of various organs, few works disclose differences between native fluorescence spectra of the cancerous and normal prostate tissues and study the biological basis of these differences. The well-known five Gleason Grades⁷ describe the evolution of malignant prostate tumor and reveal the change of prostate tissue. The pattern of Gleason Grade 1 (corresponding to early stage) consists of evenly placed uniform gland cells supported by a high, structured network of collagen fiber.^{5,7} With grade advances, the cancer cells proliferate,

the cell density increases, the cellular nuclei become non-uniform⁷ and content of collagen decreases.^{5,7} Understanding the changes during cancer evolution is critical to reveal the contributions of the key biochemical components in tissue to their fluorescence spectra.

In this study, fluorescence spectra of cancerous and normal prostate tissues with the selective excitation of 340 nm were measured to reveal changes of relative contents of key biochemical components in tissue. The intrinsic fluorescence spectra of key principle biochemical components and their contribution to entire tissue fluorescence were investigated using the method of multivariate curve resolution with alternating least squares (MCR-ALS).^{4,8} The changes of relative contents of collagen and Nicotinamide Adenine Dinucleotide (NADH) in cancerous and normal prostate tissues were observed.

2 Material and Method

Eight pairs of cancerous and normal prostate tissue samples obtained from eight different patients were provided by the Co-operation Human Tissue Network (CHTN) and National Disease Research Interchange (NDRI) under Institutional Review Board (IRB) approvals at the City College of New York. Each pair of cancerous and normal prostate tissue samples was taken from the same patient and diagnosed by a pathology medical doctor. Samples were neither chemically treated

Address all Correspondence to: Robert R. Alfano, Institute for Ultrafast Spectroscopy and Lasers Department of Physics, The City College of the City University of New York, 160 Convent Avenue, New York, New York 10031. Tel: 212-650-5533; Fax: 212-650-5530; E-mail: ralfano@sci.cuny.cuny.edu

nor frozen prior to the experiments. The time elapsed between tissue resection and measurements may have varied for different sample sources. The elapsed times were ~ 30 h. Fluorescence measurements were performed on eight pairs of cancerous and normal prostate tissue samples using a Perkin-Elmer LS-50 spectrometer. The prostate tissue samples used for fluorescence measurements were cut into $\sim 1.5 \times \sim 1 \times \sim 0.3$ cm (length \times width \times thickness) pieces. In order to study changes of the relative contents of collagen, elastin and NADH due to cancer formation, the fluorescence spectra of cancerous and normal prostate tissues were measured with the selective excitation wavelength of 340 nm, which is close to the absorption peaks of these three biochemicals. The fluorescence of other biochemicals in tissue obtained with the excitation wavelength of 340 nm is expected to have much lower intensity because their absorption peaks are far from 340 nm.

The principle method of MCR-ALS was described in detail by Tauler and de Juan.⁸ It was developed to intend the recovery of the response profile (spectra, PH profiles, time-resolved profiles, etc.) of the corresponding components in an unresolved and/or unknown mixture when no prior or little information is known about this mixture. In this study, MACR-ALS was used to extract the undistorted fluorescence spectrum of each principle biochemical component from the spectra of the prostate tissue samples and the relative contents of the principle biochemical components.

The MCR-ALS analysis is briefly described as $\mathbf{D} = \mathbf{C}\mathbf{S}^T + \mathbf{E}$, where \mathbf{D} is the data matrix containing experimental spectra in rows; \mathbf{C} is the matrix of calculated content profiles; \mathbf{S}^T is the matrix of calculated spectra of components contributed to \mathbf{D} ; and \mathbf{E} is the residual error matrix between \mathbf{D} and model $\mathbf{C}\mathbf{S}^T$. In order to obtain a physical and/or biological meaning, MCR-ALS will be achieved to approach diverse constraints (nonnegativity, unimodality, selectivity, closure, etc.) using a group of methods [such as by evolving factor analysis, least-squares calculation, or principle component (PC) analysis] applied during the iterations.

3 Experimental Results and Discussions

Differences of the emission spectra between the cancerous and normal tissue samples were reproducibly observed in the spectral range from ~ 360 to ~ 580 nm. The average fluorescence spectral profiles of the cancerous (solid line) and normal (dashed line) prostate tissues obtained with the selected excitation at 340 nm are shown in Fig. 1. Each spectral profile was normalized to unit value of 1 (i.e., the sum of squares of the data elements in each emission spectra was set as 1) before taken averaging. The main emission peak of the cancerous tissue is found at 389 nm while the emission peak for the normal tissue is at 394 nm. The major difference of the fluorescence spectral profiles of the cancerous and normal tissues is the existence of a shoulder peak at ~ 440 nm for the cancerous tissue while emission intensity of normal tissue decays monotonously with the wavelength after the main peak, and there are no shoulder peaks. This difference indicates the change of fluorophore compositions in tissue during the tumor development.

To investigate which biochemical components mainly contribute to the tissue fluorescence, the absorption spectra of collagen, elastin and NADH, and the emission spectra of col-

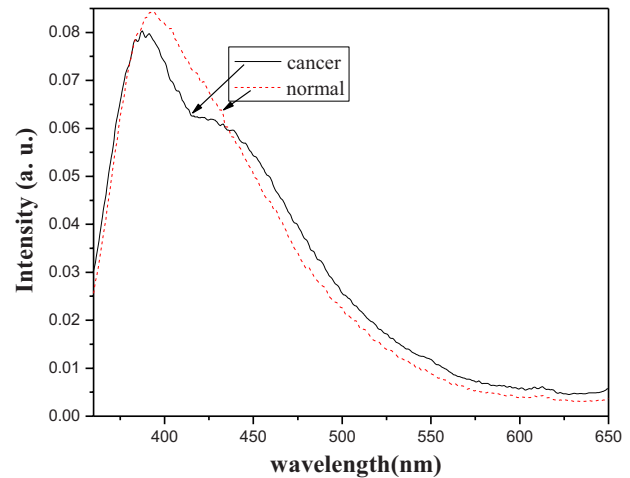


Fig. 1 Average fluorescence spectra of cancerous (solid line) and normal (dashed line) prostate tissues obtained with the selective excitation wavelength of 340 nm.

lagen, elastin NADH, and other key fluorophores (such as NAD⁺, NAD, tryptophan, and tyrosine) with the excitation at 340 nm were measured individually. The results are shown in Fig. 2. Each fluorophore was made into an aqueous solution in a quartz cell with the same concentration of ~ 0.75 mg/cm³. The fluorophore that was not soluble in water (such as collagen and elastin) was made into an aqueous suspension and shaken evenly before the measurements. The data acquisition time of each run for the fluorescence measurements is < 30 s. The absorption peaks of collagen, NADH, and elastin were observed at 339, 345, and 351 nm, respectively. The pronounced emission peaks of collagen, elastin and NADH were observed at 393, 410, and 462 nm, respectively. The emission intensities obtained with 340-nm excitation for other fluorophores are much weaker than collagen, elastin and NADH because of the absorption peaks of other fluorophores are far from 340 nm. Among these fluorophores other than collagen, elastin and NADH, tryptophan has strongest fluorescence in-

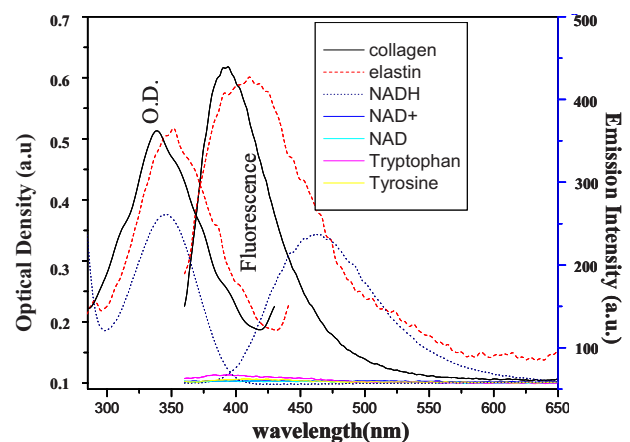


Fig. 2 Absorption spectra of three PCs of collagen, elastin and NADH, and fluorescence spectra of seven key tissue fluorophores in aqueous solution (collagen, elastin, NADH, NAD⁺, NAD, tryptophan, and tyrosine). The fluorescence spectrum of each individual fluorophore in solution was obtained using the excitation wavelength of 340 nm.

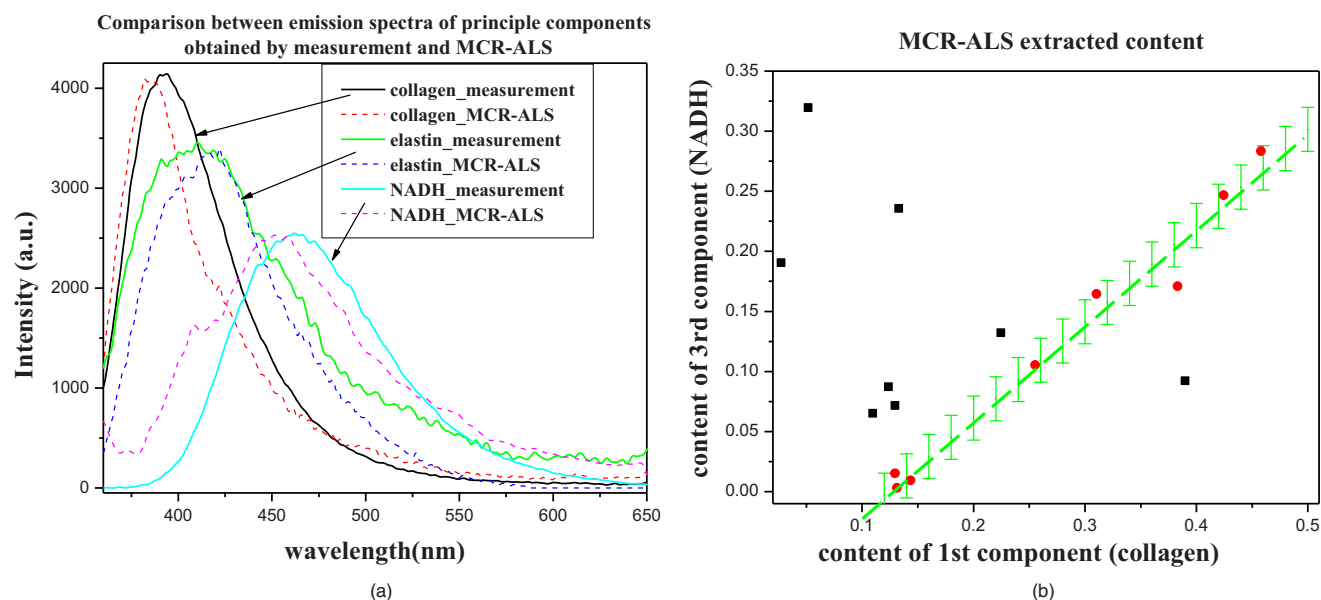


Fig. 3 (a) Comparison of spectra of three PCs (dashed line) extracted using the MCR-ALS method, and the measured (solid line) individual spectra of collagen, elastin and NADH; and (b) fractional content of the first component (collagen) versus that of the third component (NADH) obtained with the MCR-ALS method.

tensity, but its fluorescence intensity obtained with the 340-nm excitation is ~ 50 times smaller than that for collagen. Another fluorophore, flavin adenine dinucleotide (FAD), is also reported as important biomarker in tissue.⁹ However, the contribution of FAD to tissue fluorescence excited with 340 nm is much weaker than NADH because its absorption peak locates at ~ 450 nm (far from 340 nm) and emission peak is ~ 520 nm.⁹ Therefore, it is reasonable to conclude that the fluorescence profiles of cancerous and normal prostate tissues excited with 340 nm are mainly contributed from collagen, elastin and NADH, which can be regarded as three principle fluorophores. The MCR-ALS analysis can be used to extract both individual spectra and the relative contents of these three key principle components (fluorophores) from the entire fluorescence spectra of tissue obtained with the 340-nm excitation.

In the MCR-ALS analysis, eigenvalues and eigenspectra for cancerous and normal prostate tissues were calculated. The leading three PCs of collagen, elastin and NADH were accounted as 99.8% of the total variance, and coefficient of determination is found to be 99.6%. This means using one more extra component (the fourth PC) does not change much in the variance than using these three PCs.

To understand the changes of relative contents of principle biochemical components in the cancerous and normal prostate tissues, the spectrum of each component and its weighted contribution to the entire tissue fluorescence spectra were extracted from the measured fluorescence spectra of the cancerous and normal prostate tissues as shown in Fig. 1 using the MCR-ALS method. The spectra of the principle fluorophores of collagen, elastin and NADH obtained using the MCR-ALS methods are shown as dashed lines in Fig. 3(a). For comparison, the individual spectra of collagen, elastin and NADH in solution were also plotted as solid lines in Fig. 3(a). These two groups of spectra show reasonable agreement with each

corresponding counterpart, which demonstrates that MCR-ALS model accounts for the major spectroscopic feature as observed. The differentiation between the extracted spectra in tissue and measured individual spectra in solution of each component was observed and mainly resulted from distortions caused by tissue scattering and absorption.^{4,6} In the case of NADH, the emission peak of “free” NADH in solution was observed at 462 nm, while the emission peak of the MCR-ALS extracted fluorescence spectrum of NADH in tissue was found at ~ 440 nm. This spectral shift was studied and attributed to different environment status: the former is NADH in solution and the latter is NADH in tissue, which includes a large contribution of protein-bound NADH. The extracted emission spectrum of NADH in tissue was obtained using the measured entire tissue fluorescence spectra as shown in Fig. 1 and the MCR-ALS analysis method. The emission spectrum of free NADH in solution was not used in MCR-ALS extraction. Therefore, the spectral shift between tissue and solution does not affect the evaluation of MCR-ALS. The relative contents of collagen, NADH, and elastin, in the cancerous and normal prostate tissues were extracted using the MCR-ALS method by treating collagen, elastin and NADH as PCs. Figure 3(b) shows the fractional content of the first component (collagen) versus the third component (NADH) of the cancerous (square) and normal (circle) tissues. The salient feature of Fig. 3(b) is that most cancerous data points locate in the upper side than the normal data (comparing them in each vertical direction with a same content of collagen), indicating that the ratio of relative contents of NADH over collagen is higher in cancerous tissue compared to normal tissue. This is in good agreement with changes of biochemical contents in tissue during evolution of prostate malignant tumor.^{5,7} It is well known that NADH mainly exists inside cells and collagen fiber is the structure network supporting the prostate tissue.⁵ In the evolution of a typical malignant tumor, it first grows in volume

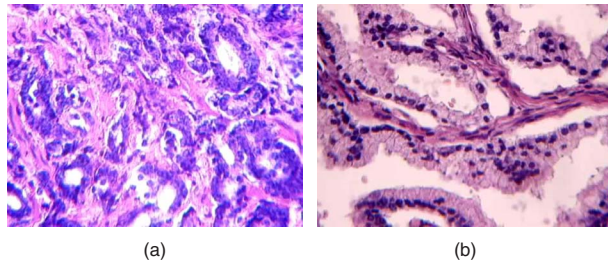


Fig. 4 (a) 40 \times magnified microscope image of a cancerous prostate tissue sample and (b) 40 \times magnified microscope image of a normal prostate tissue sample. The cancer is estimated as Gleason grade 3+4.

until it reaches some limitation of confining volume; then, the mechanical pressure increases its cell density. For prostate malignant tumors, the cancer cells proliferate, begin to merge into an “island,” and increase the cell density with nonuniform swelling cellular nuclear with grade advances.⁷ These changes of tissue structure are illustrated in Fig. 4 by the microscope images of cancerous and normal areas of one of the studied prostate tissue samples. In normal prostate tissue, the collagen network is dense with a larger number of fibers compared to nonuniform, loss, and disintegration of collagen fiber in prostatic adenocarcinoma.⁵ Because the fluorescent intensity is proportional to the fluorophores content in tissue, the reduced content of collagen and increased content of NADH exposed from their contribution to entire tissue emission may present a potential criterion for prostate cancer detection.

Another important feature shown in Fig. 3(b) is that data for normal tissue were correlated, but data for cancerous tissue is uncorrelated (i.e., the changes of relative contents of collagen and NADH are somehow related to each other for normal tissue while these changes are not related to each other for cancerous tissue). The linear dependence of data for normal tissue can be explained by the even structure of normal prostate tissue⁷ because it consists of evenly placed uniform gland cells supported by a high, structured network of collagen fiber.^{5,7} Linear regression analysis was applied for the normal tissue data to illustrate even structure of normal tissue. Linear correlation of NADH and collagen was fitted using the equation of $C_{\text{NADH}} = b \times C_{\text{collagen}} + m$. The goodness of fit of linear correlation between NADH and collagen is schematically shown as the dashed line in Fig. 3(b), which can be characterized by correlation coefficient $R^2 = 0.976$. Relative to the linear fitting line applied with error bar for normal tissue data, the cancerous and normal regions are defined. There is one cancerous datum falling below the line of normal tissue data and one normal datum out of the linearly normal region.

In a diagnosis test for cancer, the test outcome can be positive (cancer) or negative (healthy). To evaluate the potential of a diagnosis method, the following statistic terms are usually used: (1) true positive, defining as cancerous sample correctly diagnosed as malignant; (2) false positive, defining as healthy sample incorrectly identified as malignant; (3) true negative, defining as healthy sample correctly identified as healthy; and (4) false negative, defining as cancerous sample incorrectly identified as healthy. In our study, the changes of the relative contents of collagen and NADH obtained from the

measured tissue fluorescence spectra and the MCR-ALS analysis as shown in Fig. 3(b) can be used for prostate cancer detection. If we consider a higher ratio of NADH/collagen contents is related to the cancerous tissue and smaller ratio of NADH/collagen contents is related to normal tissue, the statistic terms for our data shown in Fig. 3(b) were calculated as true positive, 7; false positive, 0; true negative, 8; and false negative, 1 for the total samples of 8. The good statistic diagnosis results demonstrate that the changes of relative contents of NADH and collagen analyzed using MCR-ALS, and the fluorescence spectra obtained with selective excitation wavelength of 340 nm may be used as a biomarker for detection of prostate cancer.

The changes of relative contents of NADH and collagen may also be directly exposed from fluorescence spectra of the cancerous and normal prostate tissues using the fluorescence intensities at their fingerprint spectral peaks. The peak emission intensities of collagen and NADH were obtained from fluorescence spectra of each pair of the cancerous and normal tissues. Figure 5(a) shows the intensity at characteristic fluorescence peak of NADH versus that of collagen obtained from normalized fluorescence spectra of the cancerous (square) and normal (circle) tissues. It can be seen that five cancerous tissue data points locate in the upper side than normal tissue data. It is expected and caused by the increased cell density⁷ and loss of collagen fiber in prostatic adenocarcinoma.⁵ Linear regression was applied for the normal tissue data to evaluate the correlation of NADH and collagen contents in normal tissue and the fitting results plotted as a dashed line in Fig. 5(a). The correlation coefficient is obtained as $R^2 = 0.70$. It is clear that one datum point for normal tissue is outlier from others (the ratio of $I_{\text{peak}}^{\text{NADH}} / I_{\text{peak}}^{\text{collagen}}$ is smaller than others), and the remaining points are inside the error bar range of the normal region. Three cancerous data points fall in the normal area and can be regarded as false positive.

Because each pair of the cancerous and normal samples was taken from same patient, comparing the ratio of NADH over collagen for each pair of the cancerous and normal tissue samples may also present an extra diagnosis parameter. The ratios of intensities at the characteristic peak of NADH over that of collagen were calculated using data shown in Fig. 5(a). The ratios obtained using measured characteristic peak intensities were shown in Fig. 5(b). It can be seen from Fig. 5(b) that just two ratios for cancerous tissues are less than normal tissues.

Prostate cancer is classified as an adenocarcinoma, or glandular cancer. Because of the mean mucosa thickness of $830 \pm 60 \mu\text{m}$ and the mean rectal wall thickness of $2.57 \pm 0.15 \text{ mm}$,¹⁰ the excitation light at 340 nm cannot penetrate the rectal wall to reach prostate if irradiating from rectum. However, helped by the advancement of microendoscope (ductoscope) and fiber technology,¹¹ minimally invasive detection of prostate cancer using a tiny microendoscope directly touching the prostate gland and fluorescence difference between cancerous and normal prostate tissues may be achieved through transrectal approach with the excitation wavelength of 340 nm. Usually, the prostate biopsy needles are $\sim 1.2 \text{ mm}$ diam.¹² In contrast, researchers have provided valuable experiences in measuring fluorescence through an optical fiber of $\sim 200 \mu\text{m}$ diam.¹¹ By employing the tiny mi-

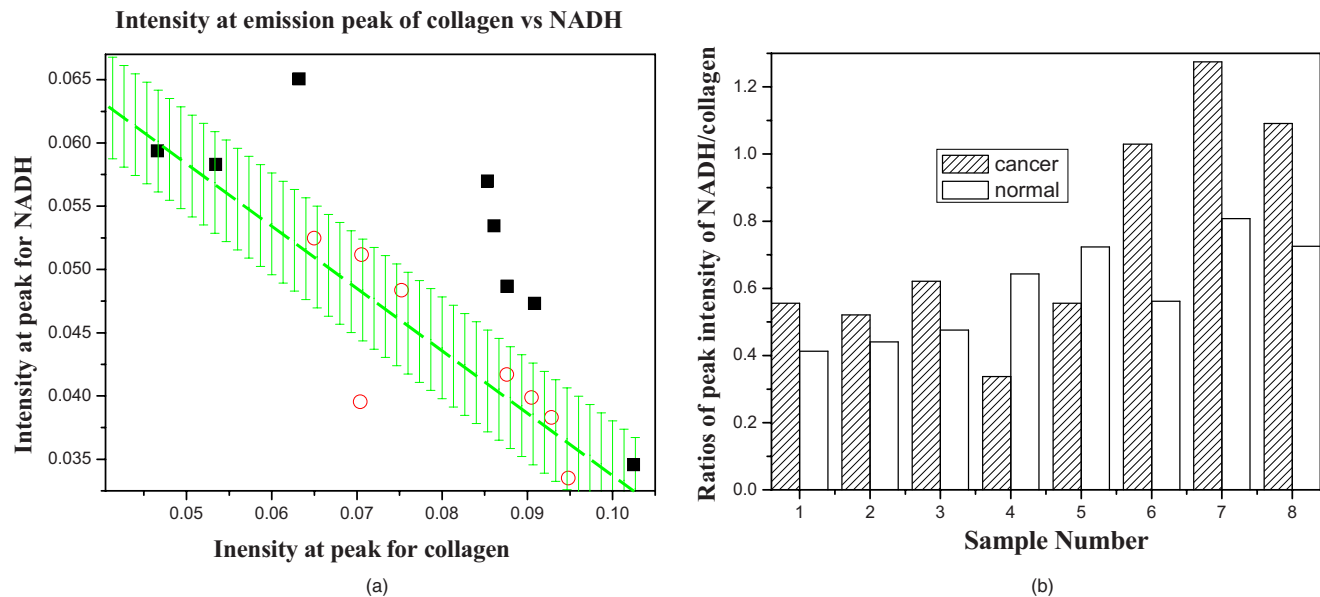


Fig. 5 (a) Fluorescence intensity at the characteristic spectral peak of NADH versus that of collagen for cancerous and normal prostate tissues obtained using our measured tissue fluorescence spectra and (b) the ratios of relative contents of NADH over collagen for cancerous and normal prostate tissues obtained using the measured data shown in (a).

croendoscope technique, this research may have positive impact in clinic applications to reduce significant pain and amount of bleeding blood for patients in prostate cancer detection.¹²

4 Conclusion

Changes of fluorescence spectra were observed in the cancerous prostate tissue compared to normal tissue. The analysis of tissue fluorescence spectra using MCR-ALS shows that the fluorescence spectra of prostate tissue obtained with the selective excitation wavelength of 340 nm are mainly contributed by three key principle biochemical components of collagen, elastin and NADH. The results indicate that the changes of fluorescence spectra of cancerous tissue compared to normal tissue are caused by reduced contribution of collagen and increased contribution of NADH. This work shows the changes of relative contents of NADH and collagen studied using fluorescence spectroscopy with the selective excitation of 340 nm may present potential criteria for prostate cancer detection.

Acknowledgments

This research is supported in part by U.S. Army Medical Research and Materiel Command under Grant No. W81XWH-08-1-0717 (CUNY RF 47170-00-01). The authors acknowledge the help of CHTN and NDRI for providing normal and cancerous prostate tissue samples for the measurements, and the help of C.-H. Liu and A. Alimova for the fluorescence spectral measurements.

References

1. American Cancer Society, *Cancer Facts & Figures 2009*, American Cancer Society, Atlanta (2009).

2. R. R. Alfano, D. Tata, J. Cordero, P. Tomashefsky, F. Longo, and M. Alfano, "Laser induced fluorescence spectroscopy from native cancerous and normal tissue," *IEEE J. Quantum Electron.* **20**, 1507–1511 (1984).
3. R. R. Alfano, G. C. Tang, A. Pradhan, W. Lam, D. S. J. Choy, and E. Opher, "Fluorescence spectra from cancerous and normal human breast and lung tissues," *IEEE J. Quantum Electron.* **23**, 1806 (1987).
4. I. Georgakoudi, B. C. Jacobson, M. G. Muller, E. E. Sheets, K. Badizadegan, D. L. Carr-Locke, C. P. Crum, C. W. Boone, R. R. Dasari, J. Van Dam, and M. S. Feld, "NAD(P)H and collagen as *in vivo* quantitative fluorescent biomarkers of epithelial precancerous changes," *Cancer Res.* **62**, 682–687 (2002).
5. C. Morrison, J. Thornhill, and E. Gaffney, "The connective tissue framework in the normal prostate, BPH and prostate cancer: analysis by scanning electron microscopy after cellular digestion," *Urol. Res.* **28**(5), 304–307 (2000).
6. R. Drezek, K. Sokolov, U. Utzinger, I. Boiko, A. Malpica, M. Follen, and R. Richards-Kortum, "Understanding the contributions of NADH and collagen to cervical tissue fluorescence spectra: modeling, measurements, and implications," *J. Biomed. Opt.* **6**(4), 385–396 (2001).
7. D. F. Gleason and G. T. Mellinger, "Prediction of prognosis for prostatic adenocarcinoma by combined histological grading and clinical staging," *J. Urol. (Baltimore)* **111**(1), 58–64 (1974).
8. R. Tauler and A. de Juan, "Multivariate curve resolution with alternating least-squares (MCR-ALS)," (<http://www.ub.edu/mcr/ntheory.htm>) (Feb. 2005).
9. D. B. Tata, M. Foresti, J. Cordero, P. Tomashefsky, M. A. Alfano, and R. R. Alfano, "Fluorescence polarization spectroscopy and time-resolved fluorescence kinetics of native cancerous and normal rat kidney tissues," *Biophys. J.* **50**, 463–469 (1986).
10. C. H. Huh, M. S. Bhutani, E. B. Farfan, and W. E. Bolch, "Individual variations in mucosa and total wall thickness in the stomach and rectum assessed via endoscopic ultrasound," *Physiol. Meas.* **24**, N15–N22 (2003).
11. I. Zeylikovich, G. C. Tang, A. Katz, Y. Budansky, and R. R. Alfano, "Fluorescence-based micro-endoscopes for breast cancer ductoscopy," *Proc. SPIE* **6091**, 609102 (2006).
12. "Men's prostate biopsy," (<http://www.articlesbase.com/advertising-articles/men039s-prostate-biopsy-1925566.html>) (Mar. 2, 2010).